Review of Computational Anthropomorphic Anatomical and Physiological Models

History, latest advances, current challenges and future prospects for computer models of anatomy and physiological functions are addressed in this review.

By Habib Zaidi, *Senior Member IEEE*, and Benjamin M. W. Tsui, *Fellow IEEE*

ABSTRACT | The widespread availability of high-performance computing and accurate and realistic computer simulation techniques has stimulated the development of computational anthropomorphic models of both the anatomy and physiological functions of humans and laboratory animals. These simulation tools have been applied to different medical imaging modalities including ultrasound, single photon emission computed tomography, positron emission tomography, X-ray computed tomography, magnetic resonance imaging, optical imaging, and multimodality imaging with various combinations of the above. This paper reviews the fundamental and technical challenges and future directions of developing computational models of normal and abnormal human anatomy and physiological functions, with a particular focus on their applications to biomedical imaging and radiation dosimetry calculations. The combination of accurate and realistic computer generated models of human and laboratory animals, radiation sources and distributions, transport of radiation through biological tissues, characteristics of the imaging system, and physics of the image formation process allows accurate and realistic simulation of biomedical imaging data and radiation dose distributions that are ever closer to those obtained from clinical and experimental laboratory animal studies. These simulation tools and techniques will provide an increasingly important contribution and impact in the future of biomedical imaging and dosimetry calculations.

Manuscript received July 20, 2009. Current version published November 18, 2009. This work was supported by the Swiss National Foundation under Grant 31003A-125246.
H. Zaidi is with the Division of Nuclear Medicine, Geneva University Hospital, CH-1211 Geneva, Switzerland and Geneva Neuroscience Center, Geneva University, CH-1211 Geneva, Switzerland (e-mail: habib.zaidi@hcuge.ch).
B. M. W. Tsui is with The Russell H. Morgan Department of Radiology and Radiological Sciences, John Hopkins Medical Institutions, Baltimore, MD 21287 USA (e-mail: btsui1@jhmi.edu).
Digital Object Identifier: 10.1109/JPROC.2009.2032852

KEYWORDS | Anthropomorphic models; human anatomy; laboratory animal anatomy; Monte Carlo simulation; radiological imaging; stylized models; voxel models; hybrid models

I. INTRODUCTION

The development of advanced methods for the design of computational models that represent the human and laboratory animal anatomy and physiology has been one of the most active areas of research in molecular imaging and radiation dosimetry [1]. Such computational models are used extensively to derive dose conversion parameters in radiation protection and nuclear medicine, to optimize imaging systems design and select the most favorable imaging protocols, and to aid in the development and performance evaluation of new image reconstruction and correction algorithms in quantitative molecular imaging [2]–[4]. The widespread availability of high-performance computing platforms and popularity of computer simulations motivated further the growth of computational anthropomorphic models corresponding to the anatomy and physiology of both humans and laboratory animals [1], [5], [6]. Such computational models are thoroughly coupled to radiation transport computer codes and accurate models of various molecular imaging modalities.

The conceptual basis lying behind the development of a physical or experimental phantom or computational model is to mimic as accurately as possible the biological and physiological properties of an organ or body region of interest or the entire body with the aim to reproduce through computer simulations the behavior of the various components of a biological system under controlled conditions [7]. In other terms, a computational model depicts mathematically an organ or tissue of the body, an organ system, or the whole body [8]. This would permit a better understanding of how radiation interacts with

biological tissues through various mechanisms of radiation interaction with matter and deposits energy (for radiation dosimetry applications) or to determine the best detection geometry configuration of a molecular imaging unit for imaging a particular region of the human body (e.g. brain, breast, prostate, etc.). Such an understanding relies on approximations regarding the chemical composition, shape, size, and possible movement of biological tissues that will be used as input to analytical or Monte Carlo simulation packages to randomly sample processes using probability density functions governing the physical system being simulated.

Simulation has become a very useful and popular research tool in molecular imaging and radiation dosimetry investigations during the last two decades owing to the more widespread availability of highly powered computing workstations and geographically distributed computing networks. Physical phantoms, although experimentally important in benchmarking the data, are considered to be impractical, time-consuming, and, in many cases, unsafe to use especially for large-scale studies involving administration of relatively large amounts of radioactivity in the phantoms, which increases the exposure of operators. Despite these limitations, many static and dynamic four-dimensional (4-D) physical anthropomorphic phantoms were recently developed in academic and corporate settings, but very few dynamic torso phantoms are commercially available. Virtually all of them were specifically designed for the assessment of renal [9] or nuclear cardiology scanning protocols and ejection fraction calculation software (e.g., the dynamic cardiac phantom available from Data Spectrum Corporation, Inc.) and as such might not be suitable for oncology-related 4-D imaging research. Some investigators designed and constructed physical phantoms that matched their own research requirements [10]–[14].

Two main classes emerged for defining anthropomorphic computational models: the stylized approach, where equation-based mathematical functions (surface equations) are used to represent the boundaries of shapes defining the model; and the voxel-based digital approach, where the object is represented by volume arrays or three-dimensional (3-D) voxel matrices. More recently, the hybrid equation-voxel approach, which combines the two approaches referenced above by allowing the mathematical description of organ boundaries from definitions extracted from voxel data, came into sight [15]–[18].

As a result of the popularity and widespread acceptance of modeling and simulation as research tools, many issues are being addressed with respect to the relevance and potential of complex anthropomorphic models, how close they are to the anatomy and physiology of patients and laboratory animals, and what the barriers are to their availability and applicability in clinical and preclinical research. Some of the articles in this Special Issue will help to answer many of these questions.

This paper reviews recent advances in computational anatomical and physiological models that made significant progress with the advent of sophisticated modeling techniques in connection with the increasing availability of computing power and the novel challenges that need addressing by novel multidimensional and multimodal molecular imaging technologies. It briefly summarizes the historical background, latest advances, and new horizons in the developments of computational anthropomorphic models, with special emphasis on those developed specifically for medical imaging research. It should be emphasized that the recommendations of the International Commission of Radiological Protection (ICRP) were followed to use the term "phantom" only for experimental physical phantoms, whereas the term "model" is used to describe a computational model that is defined on a computer system [19].

II. HISTORICAL BACKGROUND

As mentioned earlier, the difficulties associated with the use of physical phantoms representing the human anatomy within the framework of an experimental design stimulated the interest in computational models that can be defined mathematically to reproduce approximately (yet with acceptable accuracy) real-life conditions. This has become possible thanks to the accurate modeling achieved thorough knowledge of radiation interaction processes using well-established Monte Carlo techniques [20], [21].

Early computational models were historically limited to stylized models represented by regularly shaped continuous mathematical objects defined by combinations of simple surface equations (e.g. right circular cylinders, spheres, or disks). In the late 1950s, the human body was modeled by a sphere (ICRU sphere) with lots of little spherical organs. One of the first anatomical models developed specifically for the assessment of internal absorbed dose was initiated during the Manhattan Project at Los Alamos during World War II and published later by the ICRP [22]. The main spotlight at that time was radiation protection of professionally exposed workers and, to a minor degree, the general public from exposure to radiation linked to the war. It was clear at that time that the adopted anatomical model of the human body was very rudimentary, as it was constructed using a simple set of uniform spherical objects. The intended use of this report covering almost all radionuclides was radiation protection and safety of professionally exposed workers. Nevertheless, this pioneering concept was applied by the ICRP in updated evaluations for radiation workers and was also used for other applications such as internal absorbed dose calculation in nuclear medicine studies, thanks to the seminal contributions of the Medical Internal Radiation Dose (MIRD) Committee founded by the U.S. Society of Nuclear Medicine.

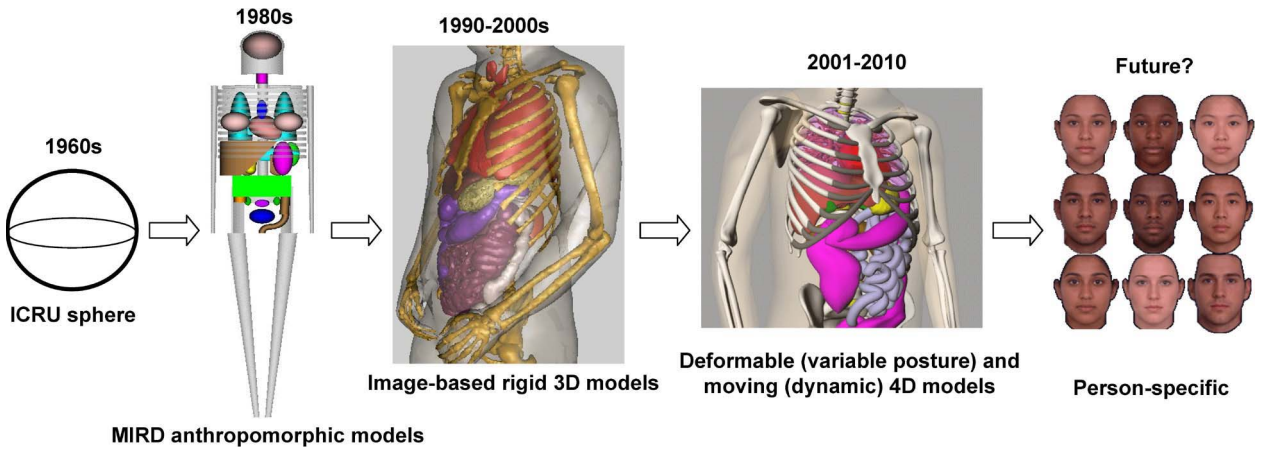

Fig. 1. *Evolution of computational models of the human anatomy from the crude ICRU spherical model to more realistic and complex (person-specific) computational models.*

The first breakthrough in the history of computational models was the development of the Fisher–Snyder heterogeneous, hermaphrodite, anthropomorphic model of the human body in the late 1960s [23]. This model and its revised version [24] were meant to represent an average adult male in good physical shape, thus portraying typical working population. The model comprised both male and female organs following the structures defined by the ICRP for the Reference Man [25], which was derived from extensive scrutinizing of medical and other literature (although limited primarily to European and North American populations). These pioneering contributions were followed by much worthwhile research efforts by academic groups and professional societies, thus allowing the development of many versatile computational models, as described in the following sections.

There was a constant desire by researchers to achieve better representations of the individual organs and the whole body in a more realistic manner. This aspiration paved the way to a series of developments that ultimately resulted in the far more realistic and sophisticated computational models available today. In essence, computational models have advanced from simple homogeneous tissue-equivalent spheres or slabs to progressively more realistic anthropomorphic models that intimately emulate the anatomy and physiology of living subjects (humans and laboratory animals). Currently available computational models belong to one of the three major categories [1]:

i) mathematical equation-based stylized models, in which organs are delineated using surface equations;
ii) image-based tomographic models, where organs are defined from segmented high-resolution medical images;
iii) equation-voxel based hybrid models, in which the mathematical description of organ boundaries is derived from definitions extracted from voxel data.

Fig. 1 illustrates the historical evolution of computational models from the crude ICRU spherical model to person-specific models expected to become available in the near future [1], [6].

III. OVERVIEW OF STYLIZED MATHEMETICAL MODELS

A. General Design Considerations

As stated earlier, stylized models are represented by regularly shaped continuous mathematical objects defined by a mixture of simple surface equations. The basic building blocks of these models consist of the usual geometrical shapes, including spheres, cylinders, ellipsoids, slabs, cones, tori, and subsections of such objects. These are usually combined to approximate the geometry of typical irregularly shaped regions of the body and its internal structures.

The representation of internal organs using simple mathematical objects is generally very crude, since simple equations can only capture the most general description of an organ's position and geometry. Such simple geometries are useful in studying fundamental issues of imaging systems' performance characteristics and dosimetry for radiation protection purposes; however, clinically realistic distributions cannot be evaluated by such simple geometries. A precise modeling of the human body requires appropriate information on the location, shape, density, and elemental composition of the organs or tissues.

B. Early Stylized Models

Early designs of computational models of the human anatomy elaborated eventually for radiation protection purposes consisted typically of homogeneous slabs, elliptical and right circular cylinders, and spheres [26], [27],

and assume a specific age, height, and weight. The large variability of individuals' bodies and internal organs results in a diversity of shapes and sizes that cannot be easily accommodated using simple models. In the 1960s, investigators from Oak Ridge National Laboratory (ORNL) reported on the development of an adult model consisting of three specific regions: the head and neck, the trunk including the arms, and the legs [28].

The major drawbacks of this model are the rough approximations utilized to represent the human body (limited to elliptical cylinders and truncated elliptical cones) and the intrinsic postulation of homogeneous tissue density and composition. In addition, some organs, such as the skeleton and the lungs, were lacking, and the geographic locations of specific organs in the model were not delineated.

These advances were supplemented with the early designs of models characterizing the pediatric population (known as the similitude pediatric models), including newborn and 1, 5, 10, and 15 years old [28]. The key weakness of these designs is the crude assumption of the formalism used to create the models, which assumes that children can be modeled as small adults and, as such, their organs are simply "smaller adult organs" [7]. In other words, these models were created by applying a series of transformations to the major axes of the Cartesian coordinate system in which the adult model referenced above was defined.

An important contribution and major step forward was the development of the Fisher–Snyder heterogeneous, hermaphrodite, anthropomorphic model of the human body [23]. This model comprised three regions—skeleton, lungs, and the remainder (soft tissue)—and was devised at ORNL for SNM's MIRD Committee. Nine years later, an improved version of the heterogeneous model was published by Snyder *et al.* [24]. This stylized model consisted of spheres, ellipsoids, cones, tori, and subsections of such objects, combined to approximate the geometry of the irregularly shaped regions of the body and its internal structures. Three main sections were used to describe analytically the model including an elliptical cylinder standing for the arms, torso, and hips; a truncated elliptical cone standing for the legs and feet; and an elliptical cylinder standing for the head and neck.

The representation of internal organs with this mathematical model is very crude, since the simple equations can only capture the most general description of an organ's position and geometry. The original model developed was intended mainly to represent a healthy average adult male, which well characterized the working population of its time. The model did have both male and female organs, but most structures represented the organs of the Reference Man [25], as defined by the ICRP from an extensive review of medical and other scientific literature, restricted primarily to European and North American populations. It should be noticed that the Reference Man was a 20–30-year-old Caucasian, 70 kg in weight and 1.70 m in height (the height was later changed to be 1.74 m).

C. Current Stylized Models

The need for complementary models arose owing to the large anatomical variability across radiation worker and nuclear medicine populations. Thanks to the efforts of the ORNL group, a series of models representing adults and the pediatric population at various ages (1, 5, 10, and 15 years) were released, with the 15-year-old model serving as a model for the adult female [29], [30]. The models were based on anthropological data (legs, trunk, and head) and age-specific organ masses of the ICRP's Reference Man [25]. The different organs of the human body are mathematically defined using second-order quadratic surface equations. For example, the right lung of the ORNL adult male model is represented by half an ellipsoid with a section removed [30]

$$\left(\frac{x+x_0}{a}\right)^2+\left(\frac{y}{b}\right)^2+\left(\frac{z-z_0}{c}\right)^2\leq 1 \text{ and } z\geq z_0.$$

The above-referenced ORNL stylized models were recently revised with the aim to use them within the MIRD dose calculation formalism [31]. These revisions updated the original models by taking advantage of recent advances in stylized models of various organs including the head, brain, kidneys, rectosigmoid colon, and extrapulmonary airways and to incorporate novel models that were overlooked in the initial design such as the salivary glands and the mucosa layer of the urinary bladder, alimentary tract organs, and respiratory airways, in addition to many other incremental improvements to the original models. Another set of computational models standing for the adult female at different stages of gestation was developed [32] to provide a framework for calculation of absorbed doses to the fetus for nuclear medicine and general health physics applications.

Following the wide adoption of the MIRD heterogeneous model, many enhancements were brought to the model soon after and documented in a series of pamphlets. In addition, based on the original descriptions, other researchers have proposed customized adaptations such as those known as the "Adam" and "Eva" models [33]. The radiation protection community relied heavily on these computational models, which effectively served as the *de facto* "standard" for many years [8], [34]. Moreover, many other models corresponding to individual organs or organ systems not included in these original models were released by the MIRD committee and other independent researchers. These include subregions of the brain [35], adult [36] and pediatric [37] head and brain models, the eye [38]–[40], the nasal cavity and major airway [41], the

peritoneal cavity [42], the prostate gland [43], bone and marrow [44], [45], gastrointestinal tract [46] and a more recent refined rectum model [47], kidney [48], spheres of varying size simulating lesions [49], [50], and many others. In particular, the availability of anthropometric data allowed the development of computational models for adults of different height, taking into account the large anatomical variability [51]–[53].

Many other stylized models have been developed specifically for the assessment of image reconstruction techniques in X-ray computed tomography (CT) and emission tomography that are not appropriate for other applications in radiological sciences. Examples of these include the two-dimensional Shepp and Logan brain model [54], which has been used extensively during the early developments of image reconstruction algorithms, and the FORBILD database developed for X-ray CT imaging research [55]. The latter family of objects comprises various organ models representing the head, abdomen, lung, thorax, hip, and jaw.

D. Dynamic (4-D) Stylized Models

Despite their limitations, stylized models are still evolving and are being constantly improved, taking advantage of the availability of more refined primitives and mathematical modeling tools. One of the limitations of the above-described models is the lack of modeling physiological motion due to cardiac and respiratory cycles inherent to living subjects. The latest advances in 4-D, i.e., 3-D spatial (x, y, z) computer models incorporating accurate modeling of time-dependent geometries (t_{geometry}), are the consequence of inevitable compromise among complexity, anatomical realism, user-friendliness, and flexibility.

Recent advances intend to develop anthropomorphic models that are flexible while allowing more accurate modeling of various patient populations. The greater levels of accuracy and precision required by emerging clinical and research applications of molecular imaging imposed more constraints with respect to the realism of physiological models used in simulation studies. Thanks to the widespread availability of computer systems with a very high computational power, the use of 4-D dynamic computational models in Monte Carlo simulations is becoming possible. One such model developed specifically for emission tomography imaging research is the Mathematical Cardiac Torso (MCAT), which is an anthropomorphic computational model developed at the University of North Carolina at Chapel Hill [56]. Using mathematical formulas, the size, shape, and configurations of the major thoracic structures and organs such as the heart, liver, breasts, and rib cage are realistically modeled for imaging purposes. Although anatomically less realistic than tomographic models derived from high-resolution CT or magnetic resonance (MR) imaging, the MCAT model has the advantage that it can be easily modified to simulate a wide variety of patient anatomies. Moreover, the model simulates a dynamic beating heart incorporating changes in myocardial wall thickness, and chamber volumes, apical movement, and heart rotation during the cardiac cycle, and was further modified later to incorporate respiratory motion [57]. Other investigators also described Monte Carlo simulations of time-dependent geometries within a single 4-D Monte Carlo simulation using the GEANT4 computer code [58]–[60]. Such features became feasible following the introduction of suitable primitives that made accurate modeling of anatomical variations and physiological motion possible. Two such primitives are superquadrics [61] and nonuniform rational B-spline surfaces (NURBS) [62] that are further described in Section V below [15]. Superquadrics are a family of 3-D objects such as superellipsoids and tori, which can be used to model efficiently a variety of anatomical structures and as such have found applications in modeling heart and thorax models in CT [63] and emission tomography [61]. It is worth emphasizing that superquadric modeling provides a more realistic visualization than quadratic modeling and a faster computation than spline methods [63]. Much worthwhile research is also being carried out to develop integrated frameworks to provide direct links between tumor growth models that could be generated within the anthropomorphic models described above, where the tumors are approximated either by analytically defined five-dimensional $(x, y, z, t_{\text{geometry}}, t_{\text{activity}})$ compartments or by compound cellular lattice inserts [64].

IV. OVERVIEW OF TOMOGRAPHIC VOXEL-BASED MODELS

A. General Design Considerations

Notwithstanding efforts to renovate the stylized models described above, the modeling of the human body using simple mathematical equations produced unrealistic anatomical geometries. The design of more realistic models has been sought since the inception of computational models; however, this became possible only after the introduction of major tomographic medical imaging modalities such as CT and MRI. Tomographic models are defined by digital (voxel-based) volume arrays from segmented high-resolution structural imaging data.

In terms of geometrical spatial representation, tomographic models are in essence different from stylized models in the sense that 3-D anatomical images consist of a digital description of the anatomy using a set of basis functions having the shape of tiny cubes called voxels (pixels in 3-D). Therefore, the voxel model contains a large number of voxels connected together to describe individual anatomical structures and organs.

It must be noted, however, that compared to medical applications where these techniques found their way to the clinic without any particular constraints, the development of tomographic models from anatomical imaging

modalities faced some exclusive and inflexible technical challenges [1].

i) Whole-body models are often required, but patient scans are usually performed for a limited portion, thus producing partial scans of the body (patient exposure due to CT examinations is substantial, and MRI is a lengthy procedure).
ii) Many individual tissues/organs should be recognized and segmented manually by experienced radiologists or automatically using dedicated software.
iii) The number of voxels and thus image data size of a whole-body tomographic model can probably be too large for a PC's memory to handle.

Despite the concerns raised regarding radiation exposure, particularly to children [65], [66], the progress in multidetector CT technology has been immense during the last two decades, allowing structural and perfusion imaging with a very high spatial and temporal resolution following introduction of CT scanners with up to 256 [67] and even 320 [68] slice capability and many novel technologies such as dual-source CT, C-arm flat-panel-detector CT, and micro-CT [69], [70]. MRI generates high-resolution anatomical and functional images offering better soft-tissue contrast resolution and a wide variety of tissue contrasts compared to CT. In addition, MRI does not use any ionizing radiation and therefore can be used without restrictions in serial studies, for pediatric cases, and in many other situations where radiation exposure is a concern. This is obviously an important consideration for the task of developing computational models of healthy subjects at various ages.

In summary, four main phases should usually be followed for the development of a voxel model:

i) acquisition of high-resolution CT or MRI data sets;
ii) classification and segmentation of the various tissues and organs through assignment of unique individual labels to each anatomical structure of interest according to the targeted application;
iii) identification of the type of biological tissue and organ and their elemental tissue compositions and mass densities using, for example, tissue characteristics from ICRU Report 46 [71] and ICRP Publication 89 [72];
iv) implementation of the computational model in a Monte Carlo package to simulate radiation transport and score quantities of interest for the task at hand (e.g., simulation of a medical imaging system, dosimetry calculations, etc).

Medical image segmentation is a relatively mature research field, and various algorithms have been developed to segment images obtained using different imaging modalities. Manual segmentation procedures performed by experienced radiologists are still used, and they tend to be laborious and time-consuming, typically taking from a few months [73] to a few years [74]. It should be emphasized that there is a lack of agreement with respect to the segmentation task since the procedure inherently entails some *a priori* knowledge of the anatomy throughout the image analysis process. For instance, CT scans of the abdomen exhibit very poor soft-tissue contrast, which makes the delineation of anatomical structures very hard, if not impossible, to achieve without the use of contrast media. Likewise, large missegmentation might occur for small anatomical structures whose size in any of the 3-D spatial directions is too small (e.g., skin < 1 mm thickness) compared to the matrix size sampling the 3-D anatomical volume (typically 2 mm voxel resolution). As a consequence, the skin layer in many computational voxels is overestimated (too thick) owing to the assignment of the top layer of the voxels to the skin. Segmentation of red bone marrow is another challenging issue that was tackled through the use of an empirical formula to calculate it (except for the VIP-Man model [75]).

While most effort devoted towards the creation of human models relied on live subjects, some groups used cadavers and animals to obtain the required anatomical information through CT or MRI and combined this with the unique anatomical information that can be extracted from color cryosections. One of the advantages of cadaver imaging is that scanning the complete body is possible at the desired slice thickness and with optimal X-ray tube settings (high kVp and mAs). One such example is the National Library of Medicine's Visible Human Project (VHP), which created anatomically comparable CT, MRI, and color cryosections [76]. This pioneering development resulted in a very high-resolution model that remained for many years the one having the smallest voxel size ($0.33 \times 0.33 \times 1$ mm^3 for the male and $0.33 \times 0.33 \times 0.33$ mm^3 for the female until the recent release of the Chinese Visible Human Project presenting a set of segmented cryosections at $0.1 \times 0.1 \times 0.2$ mm^3 voxel size for a male cadaver [77]. For many years, this model served as an excellent data source from which users have created tomographic computational models for use in medical imaging simulations for adult patients. Nevertheless, cadaver imaging has its own drawbacks, such as clinically related deformation of organs (e.g., trauma) or procedure-related issues (e.g., body preparation for imaging).

B. Current Voxel-Based Models

Tomographic or voxel-based models were introduced as early as 1984, when the first models were reported independently by two investigators [78], [79]. The former model is a representation of the head and trunk from CT scans of a female cadaver, whereas the latter reported on the development of an infant and children tomographic models [80] as well as a voxel-based representation of the physical Rando–Alderson (Radiological Support Devices, CA) physical phantom [81]. In the meantime, these

pioneering developments stimulated the emergence of a whole family of tomographic models [82], [83].

A large number of tomographic models were recently developed and will only be briefly discussed here. For a more elaborate description, interested readers could consult published reviews [1], [5] and the recent book edited by Xu and Eckerman [6] dedicated to this topic. For many reasons, adult male models were the first to be released, followed by adult female, pediatric, and pregnant woman models.

Based on the commercially available physical Hoffman 3-D brain phantom [84], a realistic brain model was created reproducing spatial distributions of typical tracers used in cerebral blood flow and metabolism studies using single-photon emission computed tomography (SPECT) and positron emission tomography (PET), providing apparent relative concentrations of four, one, and zero for gray matter, white matter, and ventricles, respectively [85]. An important contribution that crystallized the field came from Zubal *et al.*, who developed a clinically realistic head–torso model refereed to as the VoxelMan from segmented CT images of an adult living man [73]. The same group has also developed a high-resolution brain model based on an MRI scan of a human volunteer, which has been extensively used to simulate neuroimaging procedures and to provide dosimetry calculations in the head. The main anatomical structures were segmented manually by an experienced radiologist and each voxel belonging to each structure assigned a unique label. Given that the model was mainly developed for nuclear medicine imaging applications, these labels could be used to assign activity and elemental tissue composition and mass density values to each structure. The head–torso model's image data are available as a $128 \times 128 \times 246$ matrix with an isotropic resolution of 4 mm^3. This model was improved later by copying the arms and legs from the above described Visible Human model and attached them to the original torso model [86]. However, the arms of the VHP cadaver were positioned over the abdominal part, which limited the usefulness of the model for simulations of whole body scanning. This problem was tackled by mathematically straightening the arms out along the model's side [87]. Fig. 2 shows coronal images of all three versions of this model. The model was also exploited to develop a new male adult voxel model called MAX [88] by adjusting the soft-tissue organ masses to match those of the ICRP Reference Man [25] and a female adult model called FAX [89].

Another model known as NORMAN was constructed using MR images of a healthy volunteer with voxel size of $2 \times 2 \times 10$ mm^3 scaled to match the body height and weight of the original [90], [91] and new referencial [92] of the ICRP Reference Man [25]. The same group released an adult female model known as NAOMI [93] that was rescaled to match the height and weight of the ICRP reference adult female.

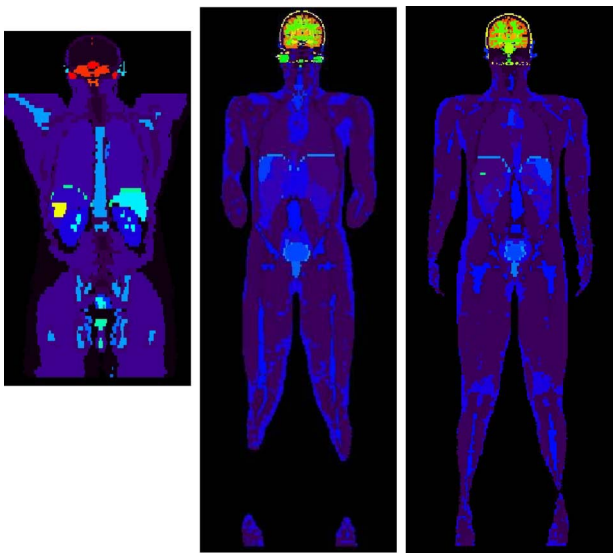

Fig. 2. *From left to right: coronal slices of the original Voxel-Man model [73], its modification by copying the arms and legs from the visible human data set and attaching them to the original model [86], and another further modification by mathematical straightening of the arms out along the model's side to make it more suitable for typical whole-body imaging simulations [87]. The data sets are available from http://noodle.med.yale.edu/phant.html.*

The German group at GSF released a "family" of nine tomographic models created from segmented CT images: BABY, CHILD, DONNA, FRANK, GOLEM, HELGA, IRENE, LAURA, and Visible Man [83], [94]. The problem with the earlier designs (e.g., GOLEM adult male model) is that they were acquired at relatively poor resolution. The BABY and CHILD models were one of the first pediatric voxel models having voxel sizes of $0.85 \times 0.85 \times 4$ mm^3 and $1.54 \times 1.54 \times 8$ mm^3, respectively [95]. A 14-year-old girl torso model called ADELAIDE was also developed using CT images [96]. Recent efforts at the University of Florida (UF) have resulted in the development of a series of partial-body (head and torso) pediatric models known as UF Series A, aging from the first year of life to 14 years old [97], [98]. These models were used to create a set of whole-body pediatric tomographic models (UF Series B) through the attachment of arms and legs from segmented CT images of a healthy Korean adult [99].

Another important contribution came from Xu *et al.*, who released an adult male tomographic model called VIP-Man based on cross-sectional cryosections of the VHP model [75]. This model consists of a huge number of voxels (3.7×10^9), where the segmentation of the original images resulted in more than 1400 tissues and organs (compared to the small number (80) considered for typical radiation dosimetry applications [75], [76]). The model is shown in Fig. 3, where 3-D surface rendering is used to illustrate anatomical realism of the trunk and

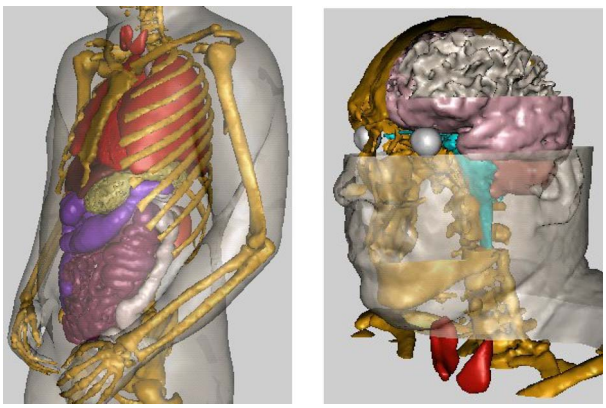

Fig. 3. *3-D surface renderings of the VIP-Man showing (left) details of internal organs and the skeleton and (right) the head and brain. (Adapted with permission from [75].)*

head, respectively. The model was recently refined (4-D VIP-Man) to incorporate respiratory motion using the NURBS primitive [100].

One interesting feature of this whole-body model is the relatively heavy body weight (103 kg) owing to the presence of a large portion of fatty tissues and, as such, was considered to be a perfect model for investigating how much a specific individual can anatomically diverge from the ICRP Reference Man [25]. One should note that most organs in both models (VIP-Man and Reference Man) have similar masses. This has stimulated the successful implementation of the model in various Monte Carlo codes including MCNP, MCNPX, EGS, and GEANT4 for internal and external dose computations entailing different particles such as photons, electrons, neutrons, and protons. The same VHP images were exploited to create the GSF's Visible Man model [101].

Several national and international initiatives were also undertaken to develop "country type" equivalents to the above-referenced VH project. In particular, many Asian countries developed their own tomographic models, including Japan [102]–[105], Korea [74], [106]–[108], and China (Visible Chinese Human and CNMAN) [77], [109], [110], and many others reportedly have similar ongoing projects.

C. Latest Developments

For more than a decade, the ICRP's Task Group on Dose Calculations and the SNM's MIRD committee have been collaborating with the aim of assessing novel dosimetry data from available tomographic models. The former was actively engaged in establishing guidelines on the use of tomographic models, suggesting the replacement of stylized models by tomographic models as early as 2002 [111]. The strategy followed by the ICRP for the development of new reference models consisted of the following steps.

1) Choose high-resolution imaging data sets of individuals close to the Reference Man in terms of height and weight.
2) Perform appropriate segmentation of the data sets.
3) Perform appropriate scaling of voxel size to adjust body height so that it matches the reference value without spoiling the realistic anatomy.
4) Perform appropriate adjustment of skeletal mass to match reference value.
5) Apply the same procedure to individual organs by addition/subtraction of voxels.

The ICRP has opted for the adjustment of the GSF models (Golem and Laura) [112] and recently released its new guidelines, emphasizing a plea for a paradigm shift from conventional stylized models to tomographic models [19]. The new ICRP reference computational models RMCP and RFCP corresponding to the Reference Adult Male and Reference Adult Female, respectively, are described in detail. Moreover, a number of new tissues and organs are now built-in in the list for the purpose of effective dose calculation for radiation protection applications.

This has also encouraged many investigators to revise early designs of tomographic models such as the MAX and FAX models that were improved to produce MAX06 and FAX06 models [113] by adjusting tissue and organ masses to match as closely as possible the anatomical values proposed in the new ICRP. Similar efforts were undertaken to adjust the NORMAN model [90], resulting in the publication of a new model called NORMAN-5 [114].

On the other hand, much worthwhile research and development efforts focused on the development of adult pregnant female models where, similar to the pediatric situation, radiation exposure due to CT examinations is a concern [16], [115]–[117]. In particular, Xu *et al.* developed an eight-month-pregnant woman model from CT images [115], which has been used to derive specific absorbed factions for nuclear medicine applications [118]. The same group released a set of pregnant female anatomic models, called RPI-P3, RPI-P6, and RPI-P9, that represent adult females at 3-, 6-, and 9-month gestational periods, respectively [119].

In addition, many other tomographic models corresponding to individual organs or organ systems not appropriately modeled using stylized models were developed independently by other research groups. These include the detailed breast model for radiological studies [120], an eye model created from the VHP female data sets [121], a series of realistic digital brain models to take into account intersubject anatomical variabilities more suitable for multimodality imaging simulations [122], and many other models.

While much effort has been devoted towards the development of human models, the need for animal

Table 1 Current Tomographic and Hybrid Preclinical Models With Their Main Characteristics

Institution	Name	Animal	Images	Reference
Johns Hopkins University, US	MOBY	Mouse	MRI	[124]
Lund University, Sweden	-	Mouse	Anatomic atlas	[125]
Memorial Sloan-Kettering Cancer Center, US	-	Mouse	MRI	[130]
Vanderbilt University, US		Mouse/ rat	CT	[126]
University of Southern California, US	Digim-ouse	Mouse	CT, PET, cryosection	[127]
University of California Los Angeles, US	-	Mouse	CT	[128]
INSERM U601, France		Mouse	cryosection	[129]
University of Science and Technology, China	-	Rat	cryosection	[131]
Japan Atomic Energy Agency, Japan	-	Frog	cryosection	[133]
University of Florida, US	UF canine	Dog	CT	[134]
University Medical Center Utrecht, The Netherlands	-	Rat brain	cryosection	[135]
University of Science and Technology, China	-	Rat	cyosection	[132]

models supporting molecular imaging research using preclinical models stimulated the development of the few animal models reported in the literature during the last decade. The recent interest in the use of mice and rats as models of human disease and related advances in multimodality molecular imaging instrumentation for biomedical research has spurred the development of realistic anthropomorphic models depicting the anatomy and physiological functions of laboratory animals. Most previously reported laboratory animal models have been stylized and mathematically based. More recent investigations report on the development of more realistic tomographic brain and whole-body models suitable for molecular imaging research, based on actual image data obtained from serial cryosections [123] or using dedicated high-resolution preclinical CT and/or MRI scanners.

Table 1 summarizes whole-body preclinical tomographic models that have been reported in the literature during the last few years. These models consist of segmented organs, and in many cases include anatomical (CT and MRI) and color cryosections that are ready for implementation into a Monte Carlo calculation code. The developed whole-body animal models include mice [124]–[130], rats [126], [131], [132], frog [133], and canine [134]. High-resolution single organ models such as the rat brain [135] were also produced.

Virtually all the models referenced above were originally created in the upright position, thus limiting the application of these models in different scenarios. In response to the lack of variable posture models, mathematical posture transformation techniques for tomographic models through a free-form deformation algorithm were suggested [105]. The technique allows the application of smooth posture transformation centering on the joints of the tomographic models while maintaining the continuity and masses of internal structures [136]. The algorithm was further refined more recently, producing improved quality of postured models [137]. Fig. 4 illustrates examples of variable posture models created from anatomically realistic tomographic models with upright standing posture.

Fig. 4. *Variable posture models developed from anatomically realistic voxel models with upright standing posture (Courtesy of T. Nagaoka, National Institute of Information and Communications Technology, Japan).*

V. OVERVIEW OF HYBRID MODELS

As indicated above, hybrid equation-voxel modeling emerged as a novel approach allowing the combination of stylized (equation-based) and tomographic (image-based) approaches by representing organ boundaries from definitions extracted from voxel data [15]–[18]. This approach allows one to take advantage of the most desirable features of the two modeling approaches referenced above. The basic modeling primitives used to define hybrid models are NURBS [62] and subdivision (SD) surfaces [138], which are widely used in computer graphics. These tools served as basis for the development of the 4-D NURBS-based cardiac–torso (NCAT) model [15]. The inclusion of accurate models of cardiac and respiratory physiology into the 4-D NCAT model was a considerable breakthrough to consider inherent cardiac and respiratory motion that was overlooked in the preceding models. NURBS-based deformation of organs during respiration is achieved through the use of time-dependent equations to manipulate surface control points. The NURBS primitives can sophisticatedly model the complex organ shapes and structures and their physiological functions, providing the foundation for a realistic anatomical and physiological model. The conceptual design of this model also served as a basis for development of the 4-D digital mouse model called MOBY [124] and the current series of 4-D extended cardiac–torso (XCAT) models [139]. The 4-D NCAT model was extensively used in cardiac imaging to generate realistic normal and pathological imaging data by generating predictive imaging data sets of a patient population with varying anatomy and with varying healthy and diseased states of the heart that provide the ground truth for evaluation and improvement of current and novel 4-D imaging techniques [140]. Similar techniques were also used in for assessment of PET image segmentation techniques in oncological imaging by incorporating lesions with clinically realistic complex shapes and nonuniform activity distributions [141], [142].

A. Advantages/Drawbacks of Hybrid Models Versus Stylized and Voxel-Based Models

Each of the three types of representation of computational models has its advantages and disadvantages. A comparison of stylized versus voxelized model representation was discussed in the literature [143]–[145] and will only be briefly reviewed here. Table 2 summarizes the advantages and disadvantages of stylized, voxel, and hybrid models considering various criteria relevant for simulation of imaging systems.

Stylized models based on geometric primitives remained anatomically unrealistic due to geometric limitation of quadratic equations. One of the disadvantages of the voxel-based approach is that inherent errors are introduced due to the model voxelization. The discretization errors inherent in the voxel-based representation may be reduced by finer sampling of the discretized models. Tomographic representation of anatomical models is known to suffer from slice-to-slice discontinuities, which are well portrayed in coronal and sagittal views. To underline the advantages of hybrid model over stylized and voxel models, Fig. 5 shows the comparison of alimentary tract models in the ORNL newborn stylized model [30], the UF newborn voxel model [97] and the UF newborn hybrid model. The voxel model is clearly an improvement over the stylized one; however, regional defects and discontinuities are clearly visible. The hybrid model represented using NURBS surfaces generated from the original voxel model and ICRP publication 89 [72] reference data (alimentary section lengths and masses of the reference newborn child) is by far more realistic and represents a substantial improvement over the previous two models [145].

Table 2 Comparison Between Stylized, Voxel, and Hybrid Computational Models in Terms of Anatomic Realism and Flexibility in Organ and Body Contour Changes

Features	Stylized	Voxel	Hybrid
Simple geometric descriptions	+++	–	+++
Realistic patient-specific anatomical descriptions	–––	++	+++
Memory requirements	+++	–––	––
Discretization errors	+++	––	+++
Modeling dynamic processes	++	––	+++
On-line Monte Carlo simulation of patient image data	–––	+++	+++
Computional burden (ray-tracing)	+++	–––	–––
Flexibility regarding organ and body contour changes	++	–––	+++
Modeling software complexity	++	–	–––

B. Design Considerations and Current Hybrid Models

The creation of a hybrid model involves three steps [145]: polygon mesh modeling, NURBS modeling, and voxelization. Structural imaging data sets or existing tomographic models are first used to develop polygon mesh models for the external body contour and internal anatomical structures. If CT or MR images are used as input, image segmentation should be used to define organ contours similar to the procedure used to create voxel models, whereas automated extraction of contours could easily be performed for existing tomographic models before they can be converted to a hybrid format. Several 3-D reconstruction software packages such as 3D-DOCTOR[1] and SURFdriver are commercially available and could be

[1]http://www.3d-doctor.com/.

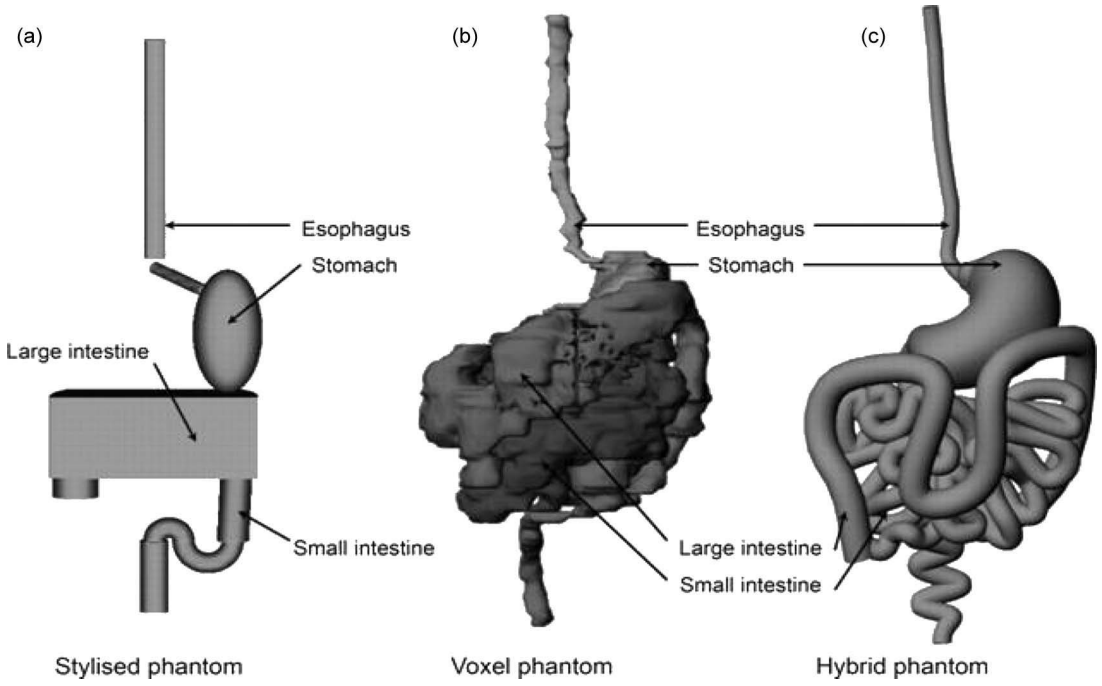

Fig. 5. *Comparison of various models of the human alimentary tract: (a) ORNL newborn stylized model, (b) UF newborn voxel model, and (c) UF newborn hybrid model. (Reprinted with permission from [145].)*

used with confidence for image segmentation and 3-D rendering. The next step consists in rendering polygon mesh models from the ensuing segmented images, which can then be exported to dedicated NURBS modeling software. NURBS-based surface models are created from the imported polygon mesh models using NURBS modeling tools, such as Rhinoceros[2] and Autodesk Maya.[3] Smooth NURBS surfaces are expanded for organ contours and organ-specific NURBS-based models generated for each tissue and organ of interest before they can be incorporated into either partial- or whole-body 3-D model framework. The technique has its limitations in the sense that NURBS surfaces are not capable of representing anatomical structures that can only be defined using a large number of parameters (e.g., some bone sites). For those structures, the original polygon mesh model is used instead. The last step consists in extracting the huge number of vertices of triangles making up body contour and internal structures from the ensuing NURBS models and in exporting for each organ to generate a voxel model suitable for use as input to a Monte Carlo radiation transport code. It should be noted that the user can choose the desired voxel resolution depending on the task at hand independently from the original imaging data or voxel model used to create the hybrid model.

Several hybrid models of humans [15]–[18], [100], [145], [146], [147] and laboratory animals [124], [132], [134] based on state-of-the-art computer graphics techniques were developed. One such example is the UF canine model shown in Fig. 6, which was designed to solve ethical issues that could stem from the use of current human dosimetry models all through novel imaging probes research. For an in-depth review of hybrid models, interested readers are encouraged to consult the detailed and comprehensive review on the subject in [139].

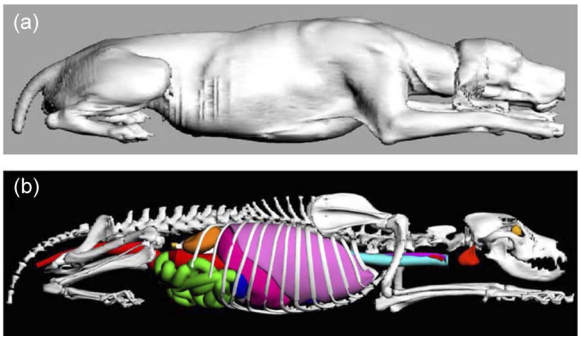

Fig. 6. *Illustration of the UF hybrid canine hybrid model. (a) Surface rendering of original CT image set and (b) NURBS surface model generated from Rhinoceros. (Adapted with permission from [134].)*

[2]http://www.rhino3d.com.
[3]http://usa.autodesk.com/.

VI. CONCLUSION AND FUTURE DIRECTIONS

It is inspiring and gratifying to see the progress that computational modeling of healthy and pathological anatomy and physiological functions of humans and animals has made, from simple spherical geometries through stylized models of reference individuals and, most recently, towards person-specific models based on patient or cadaver images. The past two decades witnessed exciting development efforts, particularly on tomographic and, more recently, hybrid models that became available through advances in medical imaging and computing technologies. To date, several voxel and hybrid models with unparalleled anatomical detail and realism have been developed for radiation dosimetry and medical imaging research.

The development and integration of realistic and subject-specific models incorporating respiratory and cardiac motion during medical imaging and radiation therapy procedures is still an open research domain [58]. Motion associated with time-varying organs involves tissue deformation, which is extremely tricky to handle using tomographic data format. The novel hybrid approach combining voxel data with NURBS and SD approaches to design even more realistic models is now taking the lead and will certainly revolutionize the application of Monte Carlo modeling techniques in clinical setting and ways of computational modeling in the same way that tomographic imaging did to the present generation of voxel models. ■

REFERENCES

[1] H. Zaidi and X. G. Xu, "Computational anthropomorphic models of the human anatomy: The path to realistic Monte Carlo modeling in medical imaging," *Annu. Rev. Biomed. Eng.*, vol. 9, pp. 471–500, 2007.

[2] H. Zaidi, "Relevance of accurate Monte Carlo modeling in nuclear medical imaging," *Med. Phys.*, vol. 26, pp. 574–608, 1999.

[3] M. Ljungberg, S.-E. Strand, and M. A. King, "Monte Carlo calculations in nuclear medicine: Applications in diagnostic imaging," in *Medical Physics Series*. Bristol, U.K.: Institute of Physics, 1998.

[4] H. Zaidi and G. Sgouros, "Therapeutic applications of Monte Carlo calculations in nuclear medicine," in *Series in Medical Physics and Biomedical Engineering*, H. Zaidi and G. Sgouros, Eds. Bristol, U.K.: Institute of Physics, 2002.

[5] M. Caon, "Voxel-based computational models of real human anatomy: A review," *Radiat. Environ. Biophys.*, vol. 42, pp. 229–235, 2004.

[6] X. G. Xu and K. F. Eckerman, *Handbook of Anatomical Models for Radiation Dosimetry*. Boca Raton, FL: CRC Press/Taylor and Francis, 2009, p. 576.

[7] J. W. Poston, W. Bolch, and L. Bouchet, "Mathematical models of the human anatomy," in *Therapeutic Applications of Monte Carlo Calculations in Nuclear Medicine*, H. Zaidi and G. Sgouros, Eds. Bristol, U.K.: Institute of Physics, 2002, pp. 108–132.

[8] ICRU, "Phantoms and computational models in therapy, diagnosis and protection," Bethesda, MD, ICRU Rep. 48, 1992.

[9] A. S. SabbirAhmed, M. Demir, L. Kabasakal, and I. Uslu, "A dynamic renal phantom for nuclear medicine studies," *Med. Phys.*, vol. 32, pp. 530–538, 2005.

[10] P. De Bondt, T. Claessens, B. Rys, O. De Winter, S. Vandenberghe, P. Segers, P. Verdonck, and R. A. Dierckx, "Accuracy of 4 different algorithms for the analysis of tomographic radionuclide ventriculography using a physical, dynamic 4-chamber cardiac phantom," *J. Nucl. Med.*, vol. 46, pp. 165–171, 2005.

[11] P. G. Begemann, U. van Stevendaal, R. Manzke, A. Stork, F. Weiss, C. Nolte-Ernsting, M. Grass, and G. Adam, "Evaluation of spatial and temporal resolution for ECG-gated 16-row multidetector CT using a dynamic cardiac phantom," *Eur. Radiol.*, vol. 15, pp. 1015–1026, 2005.

[12] R. Haddad, P. Clarysse, M. Orkisz, P. Croisille, D. Revel, and I. E. Magnin, "A realistic anthropomorphic dynamic heart phantom," *Comput. Cardiol.*, pp. 801–804, 2005.

[13] R. Haddad, I. E. Magnin, and P. Clarysse, "A new fully-digital anthropomorphic and dynamic thorax/heart model," in *Proc. Conf. IEEE Eng. Med. Biol. Soc.*, 2007, vol. 2007, pp. 6000–6003.

[14] R. Kashani, K. Lam, D. Litzenberg, and J. Balter, "Technical note: A deformable phantom for dynamic modeling in radiation therapy," *Med. Phys.*, vol. 34, pp. 199–201, 2007.

[15] W. P. Segars, "Development and application of the new dynamic NURBS-based cardiac-torso (NCAT) phantom," Dept. of Biomedical Engineering, Univ. North Carolina, Chapel Hill, 2001, p. 221.

[16] P. Dimbylow, "Development of pregnant female, hybrid voxel-mathematical models and their application to the dosimetry of applied magnetic and electric fields at 50 Hz," *Phys. Med. Biol.*, vol. 51, pp. 2383–2394, 2006.

[17] C. Lee, D. Lodwick, D. Hasenauer, J. L. Williams, and W. E. Bolch, "Hybrid computational phantoms of the male and female newborn patient: NURBS-based whole-body models," *Phys. Med. Biol.*, vol. 52, pp. 3309–3333, 2007.

[18] C. Lee, D. Lodwick, J. L. Williams, and W. E. Bolch, "Hybrid computational phantoms of the 15-year male and female adolescent: Applications to CT organ dosimetry for patients of variable morphometry," *Med. Phys.*, vol. 35, pp. 2366–2382, 2008.

[19] ICRP, "Adult reference computational phantoms ICRP," ICRP Pub. 108 (Joint ICRP/ICRU Rep.), 2009.

[20] N. Metropolis and S. Ulam, "The Monte Carlo method," *J. Amer. Stat. Assoc.*, vol. 44, pp. 335–341, 1949.

[21] S. M. Ulam, "On the Monte Carlo method," in *Symposium on Large-Scale Digital Calculating Machines*, Cambridge, MA, 1949.

[22] ICRP, "Report of Committee II on permissible dose for internal radiation," ICRP Pub. 2, 1959.

[23] W. S. Snyder, M. R. Ford, G. G. Warner, and H. L. Fisher, "MIRD Pamphlet No. 5: Estimates of absorbed fractions for monoenergetic photon sources uniformly distributed in various organs of a heterogeneous phantom," *J. Nucl. Med.*, vol. 10, pp. 5–52, 1969, suppl. 3.

[24] W. Snyder, M. R. Ford, and G. Warner, *Estimates of Specific Absorbed Fractions for Photon Sources Uniformly Distributed in Various Organs of a Heterogeneous Phantom: Pamphlet No. 5, Revised*. New York: Society of Nuclear Medicine, 1978.

[25] ICRP, "Report of the Task Group on Reference Man," ICRP Pub. 23, 1975.

[26] W. H. Ellet, A. B. Callahan, and G. L. Brownell, "Gamma-ray dosimetry of internal emitters, I. Monte Carlo calculations of absorbed dose from point sources," *Br. J. Radiol.*, vol. 37, pp. 45–52, 1964.

[27] G. L. Brownell, W. H. Ellet, and A. R. Reddy, "MIRD pamphlet No. 3: Absorbed fractions for photon dosimetry," *J. Nucl. Med.*, vol. 27, pp. 27–39, 1968.

[28] Oak Ridge National Lab., "Variation of dose delivered by 137Cs as a function of body size from infancy to adulthood," ORNL-4007, 1966.

[29] M. Cristy, "Mathematical phantoms representing children of various ages for use in estimates of internal dose," Oak Ridge National Lab., ORNL/NUREG/TM-367, 1980.

[30] M. Cristy and K. F. Eckerman, "Specific absorbed fractions of energy at various ages from internal photon sources: I methods, II one year old, III five year old, IV ten year old, V fifteen year old male and adult female, VI new-born and VII adult male, Oak Ridge National Lab.," ORNL/TM 8381/V1-V7, 1987.

[31] E. Y. Han, W. E. Bolch, and K. F. Eckerman, "Revisions to the ORNL series of adult and pediatric computational phantoms for use with the MIRD schema," *Health Phys.*, vol. 90, pp. 337–356, 2006.

[32] M. G. Stabin, E. Watson, M. Cristy, J. Ryman, K. Eckerman, J. Davis, D. Marshall, and K. Gehlen, "Mathematical models and specific absorbed fractions of photon energy in the nonpregnant adult female and at the end of each trimester of pregnancy, Oak Ridge National Lab.," ORNL/TM-12907, 1995.

[33] R. Kramer, M. Zankl, G. Williams, and D. G., "The calculation of dose from external photon exposures using reference human

phantoms and Monte-Carlo methods, Part 1: The male (ADAM) and female (EVA) adult mathematical phantoms," GSF Bericht S-885, Dec. 1982.

[34] ICRP, "Conversion coefficients for use in radiological protection against external radiation," ICRP Pub. 74, 1996.

[35] K. Eckerman, M. Cristy, and G. G. Warner, "Dosimetric evaluation of brain scanning agents," in *Proc. 3rd Int. Radiopharm. Dosim. Symp., U.S. Dept. of Health and Human Services*, Oak Ridge, TN, 1981, pp. 527–540, HHS Pub. FDA 81-8166.

[36] L. G. Bouchet, W. E. Bolch, D. A. Weber, H. L. Atkins, and J. W. Poston, "MIRD Pamphlet No. 15: Radionuclide S values in a revised dosimetric model of the adult head and brain; Medical internal radiation dose," *J. Nucl. Med.*, vol. 40, pp. 62S–101S, 1999.

[37] L. G. Bouchet and W. E. Bolch, "Five pediatric head and brain mathematical models for use in internal dosimetry," *J. Nucl. Med.*, vol. 40, pp. 1327–1336, 1999.

[38] B. L. Holman, R. E. Zimmerman, J. R. Schapiro, M. L. Kaplan, A. G. Jones, and T. C. Hill, "Biodistribution and dosimetry of N-isopropyl-p-[123] Iiodoamphetamine in the primate," *J. Nucl. Med.*, vol. 24, pp. 922–931, 1983.

[39] H. Yoriyaz, A. Sanchez, and A. dos Santos, "A new human eye model for ophthalmic brachytherapy dosimetry," *Radiat. Prot. Dosim.*, vol. 115, pp. 316–319, 2005.

[40] R. Behrens, G. Dietze, and M. Zankl, "Dose conversion coefficients for electron exposure of the human eye lens," *Phys. Med. Biol.*, vol. 54, pp. 4069–4087, 2009.

[41] H. Deloar, H. Watabe, T. Nakamura, Y. Narita, A. Yamadera, T. Fujiwara, and M. Itoh, "Internal dose estimation including the nasal cavity and major airway for continuous inhalation of C15O2, 15O2 and C15O using the thermoluminescent dosimeter method," *J. Nucl. Med.*, vol. 38, pp. 1603–1613, 1997.

[42] E. E. Watson, M. G. Stabin, J. L. Davis, and K. F. Eckerman, "A model of the peritoneal cavity for use in internal dosimetry," *J. Nucl. Med.*, vol. 30, pp. 2002–2011, 1989.

[43] M. G. Stabin, "A model of the prostate gland for use in internal dosimetry," *J. Nucl. Med.*, vol. 35, pp. 516–520, 1994.

[44] K. F. Eckerman and M. G. Stabin, "Electron absorbed fractions and dose conversion factors for marrow and bone by skeletal regions," *Health Phys.*, vol. 78, pp. 199–214, 2000.

[45] L. G. Bouchet, W. E. Bolch, R. W. Howell, and D. V. Rao, "S values for radionuclides localized within the skeleton," *J. Nucl. Med.*, vol. 41, pp. 189–212, 2000.

[46] J. W. Poston, K. A. Kodimer, and W. E. Bolch, "A revised model for the calculation of absorbed energy in the gastrointestinal tract," *Health Phys.*, vol. 71, pp. 307–314, 1996.

[47] G. Mardirossian, M. Tagesson, P. Blanco, L. G. Bouchet, M. Stabin, H. Yoriyaz, S. Baza, M. Ljungberg, S. E. Strand, and A. B. Brill, "A new rectal model for dosimetry applications," *J. Nucl. Med.*, vol. 40, pp. 1524–1531, 1999.

[48] L. G. Bouchet, W. E. Bolch, H. P. Blanco, B. W. Wessels, J. A. Siegel, D. A. Rajon, I. Clairand, and G. Sgouros, "MIRD Pamphlet No 19: Absorbed fractions and radionuclide S values for six age-dependent multiregion models of the kidney," *J. Nucl. Med.*, vol. 44, pp. 1113–1147, 2003.

[49] J. A. Siegel and M. G. Stabin, "Absorbed fractions for electrons and beta particles in spheres of various sizes," *J. Nucl. Med.*, vol. 35, pp. 152–156, 1994.

[50] M. G. Stabin and M. W. Konijnenberg, "Re-evaluation of absorbed fractions for photons and electrons in spheres of various sizes," *J. Nucl. Med.*, vol. 41, pp. 149–160, 2000.

[51] I. Clairand, L. G. Bouchet, M. Ricard, M. Durigon, M. Di-Paola, and B. Aubert, "Improvement of internal dose calculations using mathematical models of different adult heights," *Phys. Med. Biol.*, vol. 45, pp. 2771–2785, 2000.

[52] C. Huh and W. E. Bolch, "A review of US anthropometric reference data (1971–2000) with comparisons to both stylized and tomographic anatomic models," *Phys. Med. Biol.*, vol. 48, pp. 3411–3429, 2003.

[53] S. Whalen, C. Lee, J. L. Williams, and W. E. Bolch, "Anthropometric approaches and their uncertainties to assigning computational phantoms to individual patients in pediatric dosimetry studies," *Phys. Med. Biol.*, vol. 53, pp. 453–471, 2008.

[54] L. A. Shepp and B. F. Logan, "The Fourier reconstruction of a head phantom," *IEEE Trans. Nucl. Sci.*, vol. NS-21, pp. 21–43, 1974.

[55] Institute of Medical Physics, Erlangen, Germany, *The FORBILD Phantom Database*. [Online]. Available: http://www.imp.uni-erlangen.de/phantoms

[56] K. LaCroix, "Evaluation of an attenuation compensation method with respect to defect detection in Tc-99 m-sestamibi myocardial SPECT," in *Dept. of Biomedical Engineering*, Univ. of North Carolina, Chapel Hill, 1997, p. 161.

[57] W. P. Segars, D. S. Lalush, and B. M. W. Tsui, "Modeling respiratory mechanics in the MCAT and spline-based MCAT phantoms," *IEEE Trans. Nucl. Sci.*, vol. 48, pp. 89–97, 2001.

[58] H. Paganetti, "Four-dimensional Monte Carlo simulation of time-dependent geometries," *Phys. Med. Biol.*, vol. 49, pp. N75–N81, 2004.

[59] H. Paganetti, H. Jiang, J. A. Adams, G. T. Chen, and E. Rietzel, "Monte Carlo simulations with time-dependent geometries to investigate effects of organ motion with high temporal resolution," *Int. J. Radiat. Oncol. Biol. Phys.*, vol. 60, pp. 942–950, 2004.

[60] J. Zhang, X. G. Xu, C. Shi, and M. Fuss, "Development of a geometry-based respiratory motion-simulating patient model for radiation treatment dosimetry," *J. Appl. Clin. Med. Phys.*, vol. 9, pp. 16–28, 2008.

[61] J. Peter, D. R. Gilland, R. J. Jaszczak, and R. E. Coleman, "Four-dimensional superquadric-based cardiac phantom for Monte Carlo simulation of radiological imaging systems," *IEEE Trans. Nucl. Sci.*, vol. 46, pp. 2211–2217, 1999.

[62] L. Piegl and W. Tiller, *The NURBS Book*. New York: Springer-Verlag, 1997.

[63] J. Zhu, S. Zhao, Y. Ye, and G. Wang, "Computed tomography simulation with superquadrics," *Med. Phys.*, vol. 32, pp. 3136–3143, 2005.

[64] J. Peter and W. Semmler, "Integrating kinetic models for simulating tumor growth in Monte Carlo simulation of ECT systems," *IEEE Trans. Nucl. Sci.*, vol. 51, pp. 2628–2633, 2004.

[65] D. J. Brenner and E. J. Hall, "Computed tomography-an increasing source of radiation exposure," *New Eng. J. Med.*, vol. 357, pp. 2277–2784, 2007.

[66] R. Fazel, H. M. Krumholz, Y. Wang, J. S. Ross, J. Chen, H. H. Ting, N. D. Shah, K. Nasir, A. J. Einstein, and B. K. Nallamothu, "Exposure to low-dose ionizing radiation from medical imaging procedures," *New Eng. J. Med.*, vol. 361, pp. 849–857, 2009.

[67] S. Mori, M. Endo, T. Tsunoo, S. Kandatsu, S. Tanada, H. Aradate, Y. Saito, H. Miyazaki, K. Satoh, S. Matsushita, and M. Kusakabe, "Physical performance evaluation of a 256-slice CT-scanner for four-dimensional imaging," *Med. Phys.*, vol. 31, pp. 1348–1356, 2004.

[68] R. Klingebiel, E. Siebert, S. Diekmann, E. Wiener, F. Masuhr, M. Wagner, H.-C. Bauknecht, M. Dewey, and G. Bohner, "4-D Imaging in cerebrovascular disorders by using 320-slice CT: Feasibility and preliminary clinical experience," *Acad. Radiol.*, vol. 16, pp. 123–129, 2009.

[69] W. A. Kalender, "X-ray computed tomography," *Phys. Med. Biol.*, vol. 51, pp. R29–R43, 2006.

[70] J. M. Boone, "Multidetector CT: Opportunities, challenges, and concerns associated with scanners with 64 or more detector rows," *Radiology*, vol. 241, pp. 334–337, 2006.

[71] ICRU, "Photon, electron, proton and neutron interaction data for body tissues," Bethesda, MD, ICRU Rep. 46, 1992.

[72] ICRP, "Basic anatomical and physiological data for use in radiological protection: Reference values," *Ann. ICRP*, vol. 32, pp. 1–277, 2002.

[73] I. G. Zubal, C. R. Harrell, E. O. Smith, Z. Rattner, G. Gindi, and B. P. Hoffer, "Computerized 3-dimensional segmented human anatomy," *Med. Phys.*, vol. 21, pp. 299–302, 1994.

[74] C. H. Kim, S. H. Choi, J. H. Jeong, C. Lee, and M. S. Chung, "HDRK-Man: A whole-body voxel model based on high-resolution color slice images of a Korean adult male cadaver," *Phys. Med. Biol.*, vol. 53, pp. 4093–4106, 2008.

[75] X. G. Xu, T. C. Chao, and A. Bozkurt, "VIP-Man: An image-based whole-body adult male model constructed from color photographs of the Visible Human Project for multi-particle Monte Carlo calculations," *Health Phys.*, vol. 78, pp. 476–486, 2000.

[76] V. M. Spitzer and D. G. Whitlock, "The Visible Human Dataset: The anatomical platform for human simulation," *Anat. Rec.*, vol. 253, pp. 49–57, 1998.

[77] S. X. Zhang, P. A. Heng, Z. J. Liu, L. W. Tan, M. G. Qiu, Q. Y. Li, R. X. Liao, K. Li, G. Y. Cui, Y. L. Guo, X. P. Yang, G. J. Liu, J. L. Shan, J. J. Liu, W. G. Zhang, X. H. Chen, J. H. Chen, J. Wang, W. Chen, M. Lu, J. You, X. L. Pang, H. Xiao, Y. M. Xie, and J. C. Y. Cheng, "The Chinese Visible Human (CVH) datasets incorporate technical and imaging advances on earlier digital humans," *J. Anat.*, vol. 204, pp. 165–173, 2004.

[78] S. J. Gibbs, A. Pujol, Jr., T. S. Chen, A. W. Malcolm, and A. E. James, Jr., "Patient risk from interproximal radiography," *Oral Surg. Oral Med. Oral Pathol.*, vol. 58, pp. 347–354, 1984.

[79] G. Williams, M. Zankl, W. Abmayr, R. Veit, and G. Drexler, "The calculation of dose from external photon exposures using reference and realistic human phantoms and Monte Carlo methods," *Phys. Med. Biol.*, vol. 31, pp. 449–452, 1986.

[80] R. Veit, M. Zankl, N. Petoussi, and G. Drexler, "Dose equivalents in anthropomorphic phantoms and their relation to the ambient dose equivalent $H*(10)$ for external exposure," *Radiat. Prot. Dosim.*, vol. 28, pp. 29–32, 1989.

[81] R. Veit, W. Panzer, M. Zankl, and C. Scheurer, "Vergleich berechneter und gemessener Dosen an einem anthropomorphen phantom," *Z Med. Phys.*, vol. 2, pp. 123–126, 1992.

[82] M. Zankl and A. Wittmann, "The adult male voxel model 'Golem' segmented from whole-body CT patient data," *Radiat. Environ. Biophys.*, vol. 40, pp. 153–162, 2001.

[83] N. Petoussi-Henss, M. Zankl, U. Fill, and D. Regulla, "The GSF family of voxel phantoms," *Phys. Med. Biol.*, vol. 47, pp. 89–106, 2002.

[84] E. J. Hoffman, P. D. Cutler, W. M. Digby, and J. C. Mazziotta, "3-D phantom to simulate cerebral blood flow and metabolic images for PET," *IEEE Trans. Nucl. Sci.*, vol. 37, pp. 616–620, 1990.

[85] J. Kim, B. R. Zeeberg, F. H. Fahey, A. N. Bice, E. J. Hoffman, and R. C. Reba, "Three-dimensional SPECT simulations of a complex three-dimensional mathematical brain model and measurements of the three-dimensional physical brain phantom," *J. Nucl. Med.*, vol. 32, pp. 1923–1930, 1991.

[86] T. W. Dawson, K. Caputa, and M. A. Stuchly, "A comparison of 60 Hz uniform magnetic and electric induction in the human body," *Phys. Med. Biol.*, vol. 42, pp. 2319–2329, 1997.

[87] K. Sjogreen, M. Ljungberg, K. Wingardh, K. Erlandsson, and S. E. Strand, "Registration of emission and transmission whole-body scintillation-camera images," *J. Nucl. Med.*, vol. 42, pp. 1563–1570, 2001.

[88] R. Kramer, J. W. Vieira, H. J. Khoury, F. R. Lima, and D. Fuelle, "All about MAX: A male adult voxel phantom for Monte Carlo calculations in radiation protection dosimetry," *Phys. Med. Biol.*, vol. 48, pp. 1239–1262, 2003.

[89] R. Kramer, H. J. Khoury, J. W. Vieira, E. C. M. Loureiro, V. J. M. Lima, F. R. A. Lima, and G. Hoff, "All about FAX: A Female adult voxel phantom for Monte Carlo calculation in radiation protection dosimetry," *Phys. Med. Biol.*, vol. 49, pp. 5203–5216, 2004.

[90] P. J. Dimbylow, "FDTD calculations of the whole-body averaged SAR in an anatomically realistic voxel model of the human body from 1 MHz to 1 GHz," *Phys. Med. Biol.*, vol. 42, pp. 479–490, 1997.

[91] P. J. Dimbylow, "Fine resolution calculations of SAR in the human body for frequencies up to 3 GHz," *Phys. Med. Biol.*, vol. 47, pp. 2835–2846, 2002.

[92] D. G. Jones, "A realistic anthropomorphic phantom for calculating organ doses arising from external photon irradiation," *Radiat. Prot. Dosim.*, vol. 72, pp. 21–29, 1997.

[93] P. J. Dimbylow, "Development of the female voxel phantom, NAOMI, and its application to calculations of induced current densities and electric fields from applied low frequency magnetic and electric fields," *Phys. Med. Biol.*, vol. 50, pp. 1047–1070, 2005.

[94] U. A. Fill, M. Zankl, N. Petoussi-Henss, M. Siebert, and D. Regulla, "Adult female voxel models of different stature and photon conversion coefficients for radiation protection," *Health Phys.*, vol. 86, pp. 253–272, 2004.

[95] M. Zankl, R. Veit, G. Williams, K. Schneider, H. Fendel, N. Petoussi, and G. Drexler, "The construction of computer tomographic phantoms and their application in radiology and radiation protection," *Radiat. Environ. Biophys.*, vol. 27, pp. 153–164, 1988.

[96] M. Caon, G. Bibbo, and J. Pattison, "An EGS4-ready tomographic computational model of a 14-year-old female torso for calculating organ doses from CT examinations," *Phys. Med. Biol.*, vol. 44, pp. 2213–2225, 1999.

[97] J. C. Nipper, J. L. Williams, and W. E. Bolch, "Creation of two tomographic voxel models of paediatric patients in the first year of life," *Phys. Med. Biol.*, vol. 47, pp. 3143–3164, 2002.

[98] C. Lee, J. L. Williams, C. Lee, and W. Bolch, "The UF series of tomographic computational phantoms of pediatric patients," *Med. Phys.*, vol. 32, pp. 3537–3548, 2005.

[99] C. Lee, J. L. Williams, and W. E. Bolch, "Whole-body voxel phantoms of paediatric patients-UF Series B," *Phys. Med. Biol.*, vol. 51, pp. 4649–4661, 2006.

[100] X. G. Xu and C. Shi, "Preliminary development of a 4D anatomical model for Monte Carlo simulations," in *Proc. Monte Carlo 2005 Topical Meeting Monte Carlo Method: Versatility Unbounded Dyn. Comput. World*, Chattanooga, TN, Apr. 17–21, 2005.

[101] M. Zankl, U. Fill, N. Petoussi-Henss, and D. Regulla, "Organ dose conversion coefficients for external photon irradiation of male and female voxel models," *Phys. Med. Biol.*, vol. 47, pp. 2367–2385, 2002.

[102] T. Nagaoka, S. Watanabe, K. Sakurai, E. Kunieda, M. Taki, and Y. Yamanaka, "Development of realistic high-resolution whole-body voxel models of Japanese adult males and females of average height and weight, and application of models to radio-frequency electromagnetic-field dosimetry," *Phys. Med. Biol.*, vol. 49, pp. 1–15, 2004.

[103] K. Saito, A. Wittmann, S. Koga, Y. Ida, T. Kamei, J. Funabiki, and M. Zankl, "Construction of a computed tomographic phantom for a Japanese male adult and dose calculation system," *Radiat. Environ. Biophys.*, vol. 40, pp. 69–75, 2001.

[104] K. Sato, H. Noguchi, Y. Emoto, S. Koga, and K. Saito, "Japanese adult male voxel phantom constructed on the basis of CT images," *Radiat. Prot. Dosim.*, vol. 123, pp. 337–344, 2007.

[105] K. Sato, H. Noguchi, A. Endo, Y. Emoto, S. Koga, and K. Saito, "Development of a voxel phantom of Japanese adult male in upright posture," *Radiat. Prot. Dosim.*, vol. 127, pp. 205–208, 2007.

[106] C. Lee and J. Lee, "Korean adult male voxel model KORMAN segmented from magnetic resonance images," *Med. Phys.*, vol. 31, pp. 1017–1022, 2004.

[107] J. S. Park, M. S. Chung, S. B. Hwang, Y. S. Lee, D. H. Har, and H. S. Park, "Visible Korean human: Improved serially sectioned images of the entire body," *IEEE Trans. Med. Imag.*, vol. 24, pp. 352–360, 2005.

[108] C. Lee, S. H. Park, and J. K. Leec, "Development of the two Korean adult tomographic computational phantoms for organ dosimetry," *Med. Phys.*, vol. 33, pp. 380–390, 2006.

[109] B. Zhang, J. Ma, L. Liu, and J. Cheng, "CNMAN: A Chinese adult male voxel phantom constructed from color photographs of a visible anatomical data set," *Radiat. Prot. Dosim.*, vol. 124, pp. 130–136, 2007.

[110] G. Zhang, Q. Liu, S. Zeng, and Q. Luo, "Organ dose calculations by Monte Carlo modeling of the updated VCH adult male phantom against idealized external proton exposure," *Phys. Med. Biol.*, vol. 53, pp. 3697–3722, 2008.

[111] ICRP. (2002). Annual report of the ICRP. [Online]. Available: http://www.icrp.org/docs/2002_Ann_Rep_52_429_03.pdf

[112] M. Zankl, K. F. Eckerman, and W. E. Bolch, "Voxel-based models representing the male and female ICRP reference adult—The skeleton," *Radiat. Prot. Dosim.*, vol. 127, pp. 174–186, 2007.

[113] R. Kramer, H. J. Khoury, J. W. Vieira, and V. J. M. Lima, "MAX06 and FAX06: Update of two adult human phantoms for radiation protection dosimetry," *Phys. Med. Biol.*, vol. 51, pp. 3331–3346, 2006.

[114] P. Ferrari and G. Gualdrini, "An improved MCNP version of the NORMAN voxel phantom for dosimetry studies," *Phys. Med. Biol.*, vol. 50, pp. 4299–4316, 2005.

[115] C. Y. Shi and X. G. Xu, "Development of a 30-week-pregnant female tomographic model from computed tomography (CT) images for Monte Carlo organ dose calculations," *Med. Phys.*, vol. 31, pp. 2491–2497, 2004.

[116] T. Nagaoka, T. Togashi, K. Saito, M. Takahashi, K. Ito, and S. Watanabe, "An anatomically realistic whole-body pregnant-woman model and specific absorption rates for pregnant-woman exposure to electromagnetic plane waves from 10 MHz to 2 GHz," *Phys. Med. Biol.*, vol. 52, pp. 6731–6745, 2007.

[117] X. G. Xu, V. Taranenko, J. Zhang, and C. Shi, "A boundary-representation method for designing whole-body radiation dosimetry models: Pregnant females at the ends of three gestational periods—RPI-P3, -P6 and -P9," *Phys. Med. Biol.*, vol. 52, pp. 7023–7044, 2007.

[118] C. Y. Shi, X. G. Xu, and M. G. Stabin, "Specific absorbed fractions for internal photon emitters calculated for a tomographic model of a pregnant woman," *Health Phys.*, vol. 87, pp. 507–511, 2004.

[119] C. Y. Shi, X. G. Xu, and M. G. Stabin, "SAF values for internal photon emitters calculated for the RPI-P pregnant-female

models using Monte Carlo methods," *Med. Phys.*, vol. 35, pp. 3215–3224, 2008.

[120] A. K. Ma, S. Gunn, and D. G. Darambara, "Introducing DeBRa: A detailed breast model for radiological studies," *Phys. Med. Biol.*, vol. 54, pp. 4533–4545, 2009.

[121] A. A. Alghamdi, A. Ma, M. Marouli, Y. Albarakati, A. Kacperek, and N. M. Spyrou, "A high-resolution anthropomorphic voxel-based tomographic phantom for proton therapy of the eye," *Phys. Med. Biol.*, vol. 52, pp. N51–N59, 2007.

[122] B. Aubert-Broche, A. C. Evans, and L. Collins, "A new improved version of the realistic digital brain phantom," *NeuroImage*, vol. 32, pp. 138–145, 2006.

[123] F. J. Beekman and B. Vastenhouw, "Design and simulation of a high-resolution stationary SPECT system for small animals," *Phys. Med. Biol.*, vol. 49, pp. 4579–4592, 2004.

[124] W. P. Segars, B. M. Tsui, E. C. Frey, G. A. Johnson, and S. S. Berr, "Development of a 4-D digital mouse phantom for molecular imaging research," *Mol. Imag. Biol.*, vol. 6, pp. 149–159, 2004.

[125] C. Hindorf, M. Ljungberg, and S. E. Strand, "Evaluation of parameters influencing S values in mouse dosimetry," *J. Nucl. Med.*, vol. 45, pp. 1960–1965, 2004.

[126] M. G. Stabin, T. E. Peterson, G. E. Holburn, and M. A. Emmons, "Voxel-based mouse and rat models for internal dose calculations," *J. Nucl. Med.*, vol. 47, pp. 655–659, 2006.

[127] B. Dogdas, D. Stout, A. F. Chatziioannou, and R. M. Leahy, "Digimouse: A 3D whole body mouse atlas from CT and cryosection data," *Phys. Med. Biol.*, vol. 52, pp. 577–587, 2007.

[128] R. Taschereau, P. L. Chow, and A. F. Chatziioannou, "Monte Carlo simulations of dose from microCT imaging procedures in a realistic mouse phantom," *Med. Phys.*, vol. 33, pp. 216–224, 2006.

[129] A. Bitar, A. Lisbona, P. Thedrez, C. S. Maurel, D. Le Forestier, J. Barbet, and M. Bardies, "A voxel-based mouse for internal dose calculations using Monte Carlo simulations (MCNP)," *Phys. Med. Biol.*, vol. 52, pp. 1013–1025, 2007.

[130] K. S. Kolbert, T. Watson, C. Matei, S. Xu, J. A. Koutcher, and G. Sgouros, "Murine S factors for liver, spleen, and kidney," *J. Nucl. Med.*, vol. 44, pp. 784–791, 2003.

[131] L. Wu, G. Zhang, Q. Luo, and Q. Liu, "An image-based rat model for Monte Carlo organ dose calculations," *Med. Phys.*, vol. 35, pp. 3759–3764, 2008.

[132] T. Xie, W. Sun, Q. Luo, and Q. Liu, "The development of hybrid equation-voxel mouse model for Monte Carlo dose calculations," *Proc. IEEE*, vol. 97, no. 12, Dec. 2009.

[133] S. Kinase, "Voxel-based frog phantom for internal dose evaluation," *J. Nucl. Sci. Technol.*, vol. 45, pp. 1049–1052, 2008.

[134] L. Padilla, C. Lee, R. Milner, A. Shahlaee, and W. E. Bolch, "Canine anatomic phantom for preclinical dosimetry in internal emitter therapy," *J. Nucl. Med.*, vol. 49, pp. 446–452, 2008.

[135] F. J. Beekman, B. Vastenhouw, G. van der Wilt, M. Vervloed, R. Visscher, J. Booij, M. Gerrits, C. Ji, R. Ramakers, and F. van der Have, "3-D rat brain phantom for high resolution molecular imaging," *Proc. IEEE*, vol. 97, no. 12, Dec. 2009.

[136] T. Nagaoka and S. Watanabe, "Postured voxel-based human models for electromagnetic dosimetry," *Phys. Med. Biol.*, vol. 53, pp. 7047–7061, 2008.

[137] T. Nagaoka, "Voxel-based variable posture models of human anatomy," *Proc. IEEE*, vol. 97, no. 12, Dec. 2009.

[138] H. Hoppe, T. DeRose, T. Duchamp, M. Halstead, H. Jin, J. McDonald, J. Schweitzer, and W. Stuetzle, "Piecewise smooth surface reconstruction," *Comput. Graph.*, vol. 28, pp. 295–302, 1994.

[139] W. P. Segars and B. M. W. Tsui, "MCAT to XCAT: The evolution of 4-D computerized phantoms for imaging research," *Proc. IEEE*, vol. 97, no. 12, Dec. 2009.

[140] A. I. Veress, W. P. Segars, J. A. Weiss, B. M. W. Tsui, and G. T. Gullberg, "Normal and pathological NCAT image and phantom data based on physiologically realistic left ventricle finite-element models," *IEEE Trans. Med. Imag.*, vol. 25, pp. 1604–1616, 2006.

[141] S. Belhassen and H. Zaidi, "Segmentation of heterogeneous tumors in PET using a novel fuzzy C-means algorithm abstract," *J. Nucl. Med.*, vol. 50, p. 286P, 2009.

[142] A. Le Maitre, W. Segars, S. Marache, A. Reilhac, M. Hatt, S. Tomei, C. Lartizien, and D. Visvikis, "Incorporating patient specific variability in the simulation of realistic whole body ^{18}F-FDG distributions for oncology applications," *Proc. IEEE*, vol. 97, no. 12, Dec. 2009.

[143] J. Peter, M. P. Tornai, and R. J. Jaszczek, "Analytical versus voxelized phantom representation for Monte Carlo simulation in radiological imaging," *IEEE Trans. Med. Imag.*, vol. 19, pp. 556–564, 2000.

[144] A. L. Goertzen, F. J. Beekman, and S. R. Cherry, "Effect of phantom voxelization in CT simulations," *Med. Phys.*, vol. 29, pp. 492–498, 2002.

[145] C. Lee, D. Lodwick, and W. E. Bolch, "NURBS-based 3-D anthropomorphic computational phantoms for radiation dosimetry applications," *Radiat. Prot. Dosim.*, vol. 127, pp. 227–232, 2007.

[146] W. P. Segars, M. Mahesh, T. J. Beck, E. C. Frey, and B. M. W. Tsui, "Realistic CT simulation using the 4D XCAT phantom," *Med. Phys.*, vol. 35, pp. 3800–3808, 2008.

[147] J. L. Hurtado, C. Lee, D. Lodwick, T. Geode, J. L. Williams, and W. E. Bolch, "Hybrid computational phantoms representing the reference adult male and adult female: Construction and applications to retrospective dosimetry," *Health Phys.*, 2009, in press.

ABOUT THE AUTHORS

Habib Zaidi (Senior Member, IEEE) received the Ph.D. and Habilitation degrees in medical physics from Geneva University, Geneva, Switzerland.

His dissertations were on Monte Carlo modelling and quantitative analysis in positron emission tomography (PET). He is Senior Physicist and Head of the PET Instrumentation and Neuroimaging Laboratory, Geneva University Hospital, and a Faculty Member at the medical school of Geneva University. He is an Associate Professor of medical physics at the University Medical Center of Groningen, The Netherlands, and a Visiting Professor at the University of Cergy-Pontoise, France. His academic accomplishments in the area of quantitative PET imaging have been well recognized by the medical school of Geneva University, which selected him to become a Faculty Member as Privat-Docent. He is actively involved in developing imaging solutions for cutting-edge interdisciplinary biomedical research and clinical diagnosis in addition to lecturing undergraduate and postgraduate courses on medical physics and medical imaging. His research is centered on modelling nuclear medical imaging systems using the Monte Carlo method, dosimetry, image correction, reconstruction, and quantification techniques in emission tomography as well as statistical image analysis in molecular brain imaging, and, more recently, on novel design of dedicated high-resolution PET scanners in collaboration with CERN. He was a Guest Editor for three special issues of peer-reviewed journals dedicated to Medical Image Segmentation, PET Instrumentation and Novel Quantitative Techniques, and Computational Anthropomorphic Anatomical Models. He is an Associate Editor, member of the editorial board, and Scientific Reviewer for leading journals in medical physics, nuclear medicine, and scientific computing. He is a Vice Chair of the Professional Relations Committee of the International Organization for Medical Physics in addition to being affiliated with several international medical physics and nuclear medicine organizations. He is involved in the evaluation of research proposals for European and international grant organizations and participates in the organization of international symposia and top conferences as a member of scientific committees. He has been an invited speaker of many keynote lectures at an international level; has authored more than 200 publications, including high-ranking peer-reviewed journal articles, conference proceedings, and book chapters; and is the editor of three textbooks on therapeutic applications of Monte Carlo calculations in nuclear medicine, quantitative analysis in nuclear medicine imaging and multimodality molecular imaging of small animals.

Dr. Zaidi has received many awards and distinctions, including the 2003 Young Investigator Medical Imaging Science Award from the IEEE Nuclear Medical and Imaging Sciences Technical Committee, the 2004 Mark Tetalman Memorial Award from the Society of Nuclear Medicine, and the 2007 Young Scientist Prize in Biological Physics from the International Union of Pure and Applied Physics for "outstanding accomplishments in the application of biological physics to the field of medical imaging."

Benjamin M. W. Tsui (Fellow, IEEE) received the B.Sc. degree in physics from Chung Chi College, Chinese University of Hong Kong, in 1970. He received the A.M. degree in physics and Ph.D. degree in medical physics from the University of Chicago, Chicago, IL, in 1972 and 1977, respectively.

He was with the Department of Radiology, University of Chicago, from 1977 to 1982. He joined the Department of Radiology and the Department of Biomedical Engineering, University of North Carolina at Chapel Hill, in 1982 and established a Medical Imaging Research Laboratory, which focused its research on medical imaging including nuclear medicine and magnetic resonance imaging with emphasis on single photon emission computed tomography (SPECT). Also, he directed and taught in a graduate-level training program in medical imaging. In 2002, he and his laboratory joined the Russell H. Morgan Department of Radiology and Radiological Science, The Johns Hopkins University, and established a new division of Medical Imaging Physics. He became Director of the new division, which focused on research and education in medical imaging physics, especially in the areas of X-ray and nuclear medicine imaging. His research interests are in medical imaging theory, quantitative image reconstruction methods, Monte Carlo simulation, computer phantom development, image evaluation, and clinical applications in cardiac and oncological SPECT. He is the Principal Investigator of several National Institutes of Health research grants and industrial research contracts and has trained more than 30 M.S. and Ph.D. students and postdoctoral fellows. He is active in several professional societies, including the Society of Nuclear Medicine, American Association of Nuclear Cardiology, and American Association of Physicists in Medicine, and editorial boards including *Physics in Medicine and Biology* and the *Journal of Nuclear Cardiology*.

He is a Fellow of the Institute of Physics and the American Institute for Medical and Biological Engineering.